ELSEVIER

Clinical Neurophysiology 116 (2005) 718–728

www.elsevier.com/locate/clinph

Electrical brain-stimulation paradigm for estimating the seizure onset site and the time to ictal transition in temporal lobe epilepsy

S. Kalitzin*, D. Velis, P. Suffczynski, J. Parra, F. Lopes da Silva

Medical Physics Department, Dutch Epilepsy Clinics Foundation, Achterweg 5, 2103 SW Heemstede, The Netherlands

See Editorial, pages 716–717

Abstract

Objective: To explore and validate a novel stimulation and analysis paradigm proposed to monitor spatial distribution and temporal changes of the excitability state in patients with temporal lobe epilepsy (TLE).

Methods: We use intermittent pulse stimulation in the frequency range 10–20 Hz. A quantitative measure of spectral phase demodulation, the relative phase clustering index (rPCI) was applied to the evoked EEG signals, measured from electrodes implanted in the hippocampal formation.

Results: We found that in the interictal periods, high values of rPCI recorded from specific sites were correlated with the most probable seizure onset sites (SOS). Furthermore we found that high values of rPCI from certain locations correlated with shorter time intervals to the next seizure.

Conclusions: Our clinical findings indicate that although the precise moment of ictal transitions is in general unpredictable, it may be possible to estimate the probability of occurrence of some epileptic seizures.

Significance: The use of the rPCI for probabilistic forecasting of upcoming epileptic seizures is warranted. rPCI measurements may be used to guide interventions with the aim of modifying local tissue excitability that ultimately might prevent ictal transitions.

Keywords: Epilepsy; Seizure prediction; Electrical brain-stimulation; Phase coherency

1. Introduction

Epilepsy is a disease that features rapid or gradual transitions from a 'normal' functional state of the brain to an 'epileptic' state. These transitions in the majority of cases are not related to a particular known factor and are not governed by a regular time schedule. We refer therefore to the epileptic disorder as a 'dynamical disease' (Lopes da Silva et al., 2003). There has been a long-standing discussion in the literature (de Curtis and Avanzini, 2001) on the issue of relating interictal neuronal activity and any sort of forecasts concerning time, location and type of epileptic activity in patients and experimental animal models. The challenge of predicting the exact time and/or location of an epileptic seizure onset has been taken by many researchers in the recent years. The literature and variety of methods (Iasemidis, 2003; Lehnertz et al., 2003; le Van Quyen et al., 2000; Mormann et al., 2003; Worrell et al., 2004) is growing, but to our best knowledge no single technique has been validated to give definite answer to those problems. Some of the claimed results have been challenged (Aschenbrenner-Scheibe et al., 2003; Lai et al., 2003) which makes the issue even more controversial. Most studies with this objective have been carried out using spontaneous EEG signals, although Wilson et al. (1998) have used field evoked potentials as a measure of the excitability state of local neuronal networks in the limbic system. We assumed that it would be possible to obtain relevant information about the dynamical state of these networks through the analysis of activities evoked by local stimulation with pulse trains. We searched for the information in the phase domain of these evoked activities, inspired by our finding in photosensitive

* Corresponding author. Tel.: +31 235588248; fax: +31 235588119.
E-mail address: skalitzin@sein.nl (S. Kalitzin).

1388-2457/$30.00
doi:10.1016/j.clinph.2004.08.021

patients where the enhancement of phase clustering (rPCI) of some frequency components was shown to anticipate the transition to an epileptic seizure during intermittent light stimulation (Kalitzin et al., 2002; Parra et al., 2003).

We first attempt to identify the site of ictal onset in patients with TLE, undergoing invasive presurgical diagnostic evaluation. We use a particular measure of phase demodulation, the rPCI, measured interictally during intermittent electrical stimulation. The second objective is to explore the possibility and to present a 'proof-of-principle' for this methodology with respect to seizure prediction. We should note that the question of seizure prediction suffers from a fundamental imprecision: what does one precisely mean by saying that an ictal transition can be predicted? We propose here that this imprecision can be removed by using a probabilistic formulation. This means that an operational definition of seizure anticipation should be based on the probability distribution of a given measure related to the distribution of time intervals between the moment of estimation of this measure and the moment of seizure onset. We can assess the predictive value of such distribution and therefore define quantitatively seizure 'predictability'. According to this concept, predictability does not translate directly into a well-defined time of forecasting an ictal transition, it rather consists of an estimate of the chance of a seizure occurring during a certain period in the future relative to a particular moment of observation.

2. Methods

2.1. Patients and implantation

All 6 patients participating in this study were candidates for resective epilepsy surgery who underwent phase 2 invasive EEG monitoring because of lack of congruence of non-invasive presurgical evaluation studies (Dutch Collaborative Epilepsy Surgery Program, 1993). No other selection criterion applied and all patients implanted from 2001 onwards participated in the present study. Implantation was carried out through two frontal parasagittal circular craniotomies 3 cm in diameter in case of bilateral or through a single craniotomy in case of a unilateral implantation. The order of implantation and use of electrodes was determined in consultation with one of us (DV). Several semirigid subdural reeds (see Fig. 1) consisting of 5–7 (mostly 7) contacts each were inserted freehand under fluoroscopy in each implanted patient such as to cover the frontal and temporal convexities by advancing the tips of those subdural reeds to reach the orbitofrontal and the basal temporal neocortical areas. Stereotaxic insertion of depth electrodes consisting of 6 contacts each targeting the body of the hippocampus (Leksell frame, MRI guidance) was then carried out during the same session (Van Veelen et al., 1990). Video/EEG

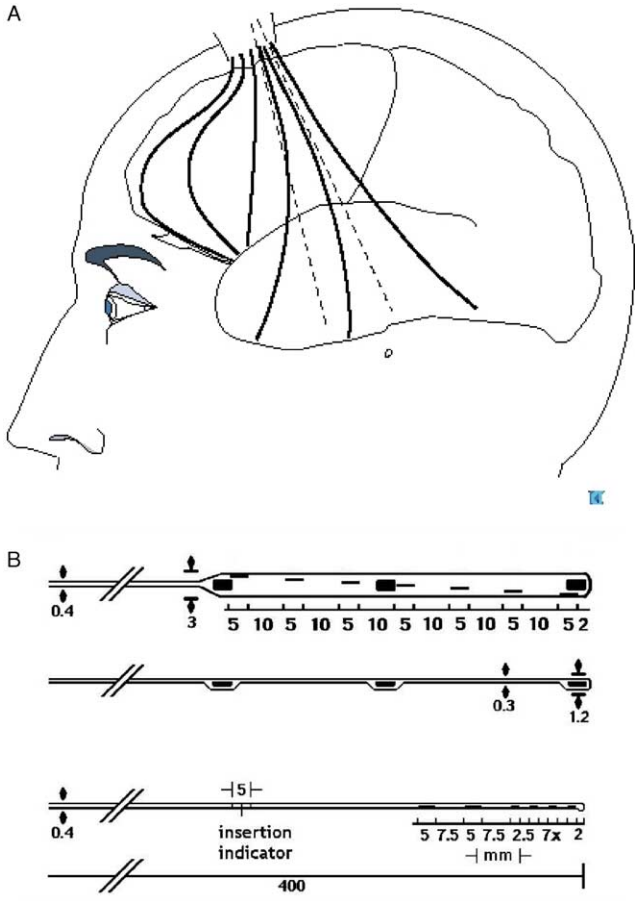

Fig. 1. Implantation layout and electrode contact designation. (Panel A) Illustrations of electrodes used, implantation scheme, and trajectories followed by subdural reeds and intracerebral electrode bundles. Solid lines indicate subdural reeds. Broken lines indicate intracerebral electrode bundle for different targets. The anterior target is the head of the hippocampus. Posterior target is the midportion of the body of the hippocampus. Note that the subdural reeds introduced to cover the temporal lobe curve around the inferior temporal gyrus and reach to the parahippocampal gyrus on the inferior and basal temporal cortex. The subdural reeds introduced to cover the frontal lobe curve around the convexity and reach the inferior and basal frontal areas. (Panel B) The geometry of the subdural reeds (top illustration) and the intracerebral electrode bundles (middle and bottom).

recording was carried out in our institution's standard epilepsy monitoring unit (EMU) environment. AED medication was tapered in order to record a sufficient number of habitual seizures for lateralization and localization of the seizure onset sites (SOS) in each patient (Van Emde Boas et al., 1990). Informed consent was obtained prior to performing the intracranial electrical stimulation studies (ICES) that we carried out while waiting for the habitual seizures to occur under supervision of one experienced EEGer (DV), who also determined SOS in all cases.

We summarise the notations in Table 1 that specify the electrode contacts. For the results in this article we used only the hippocampal contacts which will be denoted as HCL for the left hippocampus and HCR for the right

Table 1
Seizure onset site (SOS) determined by interictal rPCI (measurements taken at more than 24 h before next seizure) and seizure anticipation performance of rPCI

Patients/ gender	Video/SEEG seizure onset types	SOS at UEO	Interictal rPCI P50 [P05 P95] (contact)	Interictal lateralization p(rPCIsos> rPCIcontra)	h^2 (N, NS) [stim. frequency]
p1/M	Several widespread neocortical and mesial right temporal seizure onsets	Several contacts, most pronounced: HCR 5, HCR 7	0.54 [0.17 0.72] (HCR 5)* 0.08 [0.03 0.18] (HCR 7)	$P<0.001$	NA
	Single focal mesial left temporal seizure onset		0 [0 0.003] (HCL 5) 0 [0 0.03] (HCL 7)		
p2/F	Local mesial and neocortical right temporal seizure onset	HCR 5, HCR6	0.21 [0.13 0.29] (HCL 4) 0.04 [0.04 0.04] (HCL 7) 0.28 [0.25 0.32] (HCR 6)*	$P<0.001$	NA
p3/F	Widespread mesial and neocortical right temporal seizure onset	HCR 7	0.03 [0.0 0.2] (HCR 4) 0.31 [0.01 0.6] (HCR 7)*	NA	0.708 (769, 14) [20 Hz]* 0.713 (547, 14) [20 Hz]*
p4/M	Focal mesial right temporal seizure onset	HCR 6, HCR 7	0.26 [0.24 0.39] (HCR 6)* 0.2 [0.1 0.34] (HCR 7) 0.09 [0.04 0.23] (HCL 6)	$P<0.001$	0.045 (227, 5) [20 Hz] 0.044 (240, 5) [20 Hz] 0.428 (291, 5) [20 Hz]*
p5/F	Focal mesial left temporal seizure onset	HCL 7 more than HCL 5	0.51 [0.047 0.67] (HCL 5)* 0.2 [0.028 0.38] (HCL 7) 0.11 [0 0.42] (HCR 6) 0.0 [0 0.15] (HCR 7)	$P<0.001$	0.050 (249, 1) [15 Hz] 0.039 (344, 1) [10 Hz] 0.275 (553, 1) [15 Hz]* 0.461 (146, 1) [15 Hz]*
p6/F	Widespread neocortical right temporal and parietal seizure onset	Extra hippocampal	0.11 [0 0.77] (HCL 6) 0.168 [0 0.67] (HCR 6)	NA	NA

The first column identifies the individual patients, the second column describes the EEG findings from ictal EEG and clinical status. The third column extracts the SOS information at the Unequivocal Electrographic Onset (UEO) as found from visual inspection of preictal and ictal EEG recordings. The 4th column gives the median rPCI (P50) and the 5 and 95% percentiles for the rPCI for all the available inter-ictal data for each patient. Traces with median rPCI ≥ 0.25 are marked with * indicating the most probable SOS according to interictal rPCI measurments. Column 5 presents the results from the KS two-point test (see Section 2.4) validating the hypothesis that the hemisphere containing the SOS has higher interictal rPCI values than the contralateral hemisphere. The test uses all available measurements from left and right hippocampal contacts. Patient 3 was unilaterally implanted and therefore no lateralization test was possible. Available data show high interictal rPCI values at the SOS contact (HCR 7). Patient 6 was diagnosed with extratemporal SOS with no active involvement of either hippocampi. The median rPCI values from both hippocampal contacts were low in this case reflecting the clinical status. For the notation conventions used for the electrode contacts see Section 2.1. The last column indicates for the corresponding contacts of column 4 the non-linear association measure h^2 relating the values of rPCI to the time of next seizure. This analysis was done only for 3 patients (p3, 4 and 5) for which long-term chronic stimulation data was available. The number of measurements N, the number of seizures NS and the selected stimulation frequency is presented in brackets as indicated in the column header. Statistical significance at P-value 0.05 (marked with *) of the h^2 measure is assumed when the later is greater than $h_c^2(N)$ (see Section 2 for details). The traces with highest predictive power were found contralaterally to SOS for patients 4 and 5, for patient 3 with unilateral implantation the highest predictive power was detected at the contact closest to SOS.

hippocampus. In addition, we number the contacts in successive order starting from the most superficial contact. In general, an additional letter is used to indicate one of several nearly parallel electrode bundles. For example, HCR T6 denotes right hippocampus, bundle T, 6th contact from the top. We have omitted the bundle letter from our notations because for each patient the stimulation and recordings were performed on one selected electrode bundle (but involving different contacts on it).

Each electrical contact in the hippocampus used for stimulation (see illustration in Fig. 1) had a cylindrical shape 2.5 mm in length with a diameter of 0.4 mm, resulting in an area of 3 mm^2.

2.2. Stimulation and EEG acquisition

2.2.1. Stimulation hardware and calibration

All sessions were performed in our EMU where a closed-loop stimulation-acquisition system was installed. A Grass Telefactor (Astro-Med Inc., West Warwick, RI, USA) S8800 stimulator linked to two Grass Telefactor photoelectric stimulus isolation units (SIU7) with constant current output generated the pulses. A safety transformer drawing on 210/220 V, 50 Hz mains power, powered the stimulator. For each patient we performed ICES calibration during interictal periods prior to initiation of AED tapering and always several days before the first seizure following

electrode implantation did occur. ICES calibration involved contacts located within the hippocampal formation only. These contacts were the 4 most distally located ones on each hippocampal bundle, i.e. the contacts coded 4–7 (see Fig. 1 for details). In all calibration sessions the impedance between the corresponding contacts was measured from the waveforms recorded with digital storage oscilloscope (Fluke 92B, series II, Fluke Nederland B.V., Eindhoven, The Netherlands). The stimulation strength used was 1000 μA. Contact-pairs with impedance greater than 10 kΩ were not used for stimulation. The signal-to-noise ratio (see the next section) was determined by delivering current to any two of the 4 contacts while recording from the remaining two by stepwise increasing stimulation intensity from 500 to 1000 μA. This procedure was carried out during the initial calibration session, both for the presumed SOS and the contralateral hippocampal bundles, except in patient 3 who underwent a unilateral implantation only. Once we were convinced the optimal two contacts (highest signal-to-noise ratios) for recording had been identified, the actual ICES paradigm was carried out. ICES sessions typically lasted several hours at a time. In the case of patients 3, 4 and 5 ICES was administered both during daytime and at night, both while the patient was awake and when asleep. Data from those patients were used for our 'seizure-anticipation' tests. In patients 4, 5 and 6 we also used an electrical current splitter to output ICES to both hippocampi at the same time, approximately halving the current passed from the stimulus isolator units.

During the calibration sessions and some of the chronic stimulation sessions the patient was sitting next to the stimulator. In most chronic stimulation sessions patients were in their own room in the EMU, oblivious to the ICES session and protocol. No clinical signs were observed due to ICES (sub-threshold ICES).

2.2.2. Stimulation protocol and sequence control

Stimulation protocols consisted of biphasic, current-source generated electrical pulses of 500–1000 μA and of 0.1 ms per phase, inter-phase delay 0.1 ms. This resulted in electrical charges of 0.05–0.1 μC/phase and, taking into account the geometry of the stimulation contacts, charge-densities of 1.7–3.4 $\mu C/cm^2$ per phase. Those values are below the 'safe limits' known from both animal studies and patient research (Gordon et al., 1990).

The pulse-sequences were controlled from a Matlab version 6.5.1 (MathWorks Inc., Natick, MA, USA) interface software, using the data acquisition toolbox (version 1.2) driving the analog output of a NIDAQ (National Instruments Corp., Austin TX, USA) MIO 64 data acquisition card. Sequence frequencies were mostly 20 Hz (for patients 5 and 6 we used also 10 and 15 Hz). The duration of the sequences was 5 s (100 pulses in 20 Hz sessions) and the interval between them was minimal 20 s. An off-line printout (using Harmonie data reviewer, Stellate Systems, Montréal, version 5.2), of one of our stimulation sequences and EEG recordings is illustrated in Fig. 7.

2.2.3. Data acquisition

EEG data acquisition was performed through the same NIDAQ card via splitting the signal from a homemade digital telemetry routing. Sampling frequency was 1000 Hz and no data filtering was done for this application. Data collection, on-line calculation of rPCI and the postacquisition analysis were done in the same MatLab environment employed for the stimulator control. When required, our stimulation-acquisition ICES-SEEG system can operate in a 'closed-loop' mode.

Since the pulse duration used was extremely short, most often undetectable at the digitising sample frequency of our telemetry system (1000 Hz/channel, no data skew), we used a custom-made ICES 'pulse blur' to output an 'observable' trigger.

2.3. Digital data processing

2.3.1. Signal-to-noise ratio (SNR)

We controlled the SNR during the calibration ICES session to select the stimulation pairs with highest SNR. In addition, during the on-going stimulations the SNR was used to select data with high significance.

The signal-to-noise ratio, measured from a given stimulation session and from any electrical contact was computed as:

$$\mathrm{SNR}_i = \frac{\mathrm{SD}(\langle S_i^r(t)\rangle_r)_t}{\mathrm{SD}(\langle (-1)^r S_i^r(t)\rangle_r)_t}$$

where $S_i^r(t)$ is the temporal response of the ith contact to the rth stimulus of the sequence. The time runs from the time of the stimulus to either the next stimulus (e.g. 50 ms for 20 Hz stimulation sessions) or it was truncated to 50 ms during the calibration sessions. In the last cases 12 ICES pulses were administered with 1 s inter-stimulus intervals (1 Hz stimulation). The numerator in the above formula is just the standard deviation of the averaged stimulus–response and the denominator is the standard deviation of the so-called $\pm$ averaged response (only even numbers of stimuli are considered).

2.3.2. Phase modulation and rPCI

The full description of the rPCI quantity is given in our previous work (Kalitzin et al., 2002) and here we only present the relevant ideas and formulae. When subjected to a periodic, intermittent stimulation, the neuronal system will respond with an evoked EEG signal of certain frequency content. We can characterise this signal by its response-amplitudes and their fluctuations but also by the fluctuations of the phases of the harmonic response-components. These latter fluctuations measure the time-locking of the harmonic components to stimulation sequence. Our previous work has

shown (Parra et al., 2003) that when high-frequency response-components are 'more strongly' locked to the stimulus than the driving-frequency component itself, paroxysmal responses to photic stimulation can be anticipated. We defined the phase clustering index (PCI) in order to quantify the amount of phase clustering, or equivalently, the amount of time-locking of one harmonic component to the sequence of stimuli. The univariate PCI associated with electrode i and derived from the Fourier coefficients $F_i^r(\omega)$ (obtained by Fourier transformation of the response amplitudes $S_i^r(t)$) to a sequence of stimulation pulses is

$$\mathrm{PCI}_i(\omega) = \frac{\langle F_i^r(\omega)\rangle_r}{\langle |F_i^r(\omega)|\rangle_r}$$

where ω denotes frequency, in this study it is a multiple of the stimulation frequency, and the averaging $\langle\,\rangle$ takes place over all pulse-responses of the sequence labeled with r. PCI is a complex number and its amplitude, always smaller than one, indicates the degree of consistency between the phases of the individual complex amplitudes of the sequence, for each frequency and electrode contact. The phase of the PCI represents the average phase among the response amplitudes for the corresponding frequencies. The relative PCI (rPCI) is defined as the maximal difference between the absolute value of the PCI at any harmonic multiple n of the stimulation frequency and that of the stimulation frequency ω_0

$$\mathrm{rPCI}_i = \max_{n>0}(|\mathrm{PCI}_i(n\omega_0)|) - |\mathrm{PCI}_i(\omega_0)|$$

Each stimulus train of 5 s corresponds to one rPCI value per recorded trace. In our analysis we selected response amplitudes with signal-to-noise ratio greater than 6. For interictal analysis we selected data measurements that were collected more than 24 h before the first seizure of the patient in our facility. For the assessment of the predictive power of rPCI we selected only those traces (and stimulation frequencies, if more than one was available) that provided >100 measurement points (N in the last column of Table 1). These criteria excluded only one contact (p4, HCL 7). Given the limitations of our acquisition system we limited the analysis to harmonic components of up to 250 Hz (e.g. for stimulation with 20 Hz, the maximal harmonic number is $n=12$). In all frequency-related analysis the 50 Hz component and its multiples (100 Hz, 150 Hz, etc.) were excluded to avoid possible main's interference.

2.4. Statistical analysis

To compare the rPCI measurements at different sites and hemispheres we used interictal data. We applied single-sided two-point Kolmogorov–Smirnov (KS) comparison test as provided by the Matlab statistical toolbox. We tested the null-hypothesis (H0) that rPCI values at any contact in the hemisphere containing SOS and at any contact in the contralateral hemisphere are equally distributed versus the alternative hypothesis (H1) that rPCI(SOS)$>$ rPCI(contralateral).

To assess the time-predictive power of rPCI (measured for any electrode trace and stimulation frequency) we used a non-linear regression technique (Lopes da Silva et al., 1989; Pijn et al., 1990). For each measurement point at time t_a we collected $Q_a \equiv \mathrm{rPCI}(t_a)$ and the time interval to the next following seizure of the patient T_a. In this way a set of measurements $\{T_a\}$, $\{Q_a\}$ was obtained. We assessed the predictability power of the rPCI corresponding to a given measurement set as $\Phi = h^2(\{Q_a\}, \{T_a\})$ where $h^2(x, y)$ is the non-linear and non-symmetric regression coefficient between statistical variables x and y. Applied to our set of measurements h^2 was calculated as follows

$$h^2(\{Q_a\},\{T_a\}) = 1 - \frac{\frac{1}{N}\sqrt{\sum_q N_q^2\,\mathrm{SD}(T_a|Q_a \in [q, q+\delta q])^2}}{\mathrm{SD}(\{T_a\})}$$

where SD is standard deviation, N_q are the number of measurements of rPCI values between q and $q+\delta q$ and N is the total number of measurements. The above method depends on selecting the bin-size δq for the variable $0<Q<1$. We took for the bin-size the value of 0.1 (10 bins in total). In Table 1, the last column, the h^2 quantity is presented for all patients at different contact sites, graphical illustration is presented in Fig. 4, panel C and Fig. 5, panel A. We derived also a test for the statistical significance of the h^2 quantity depending on the number of measurement points. To evaluate the probability of acceptance of the null-hypothesis that rPCI is not correlated with the time to next seizure, we simulated 10,000 sequences of random numbers between 0 and 1. The length of each sequence was equal to the corresponding number of measurement points (N in the last column of Table 1). Using these numbers instead of the measured rPCI values and the original times to seizure $\{T_a\}$, we define the critical value $h_c^2(N)$ so that the probability of $(h^2 > h_c^2)$ is less than 0.05. The last probability is estimated from the simulated data. Values larger than $h_c^2(N)$ are, therefore, statistically significant at confidence level 0.05.

To explore further the issue of predictability we define the function

$$E(Q_c, T_c) = \frac{\#\{t_a|(Q_a > Q_c)\&(T_a > T_c)\} + \#\{t_a|(Q_a \le Q_c)\ \&\ (T_a \le T_c)\}}{\#\{t_a\}}$$

where $\#\{\ \}$ is the number of elements in a given set, T_c is a running prediction horizon and Q_c is a running rPCI threshold. The above equation represents the relative number of false predictions under the assumption that the following seizure will occur earlier than T_c if rPCI

(denoted as Q_a) is larger that Q_c and vice versa. The first term in the numerator above gives the number of the false positive predictions and the second term represents the number of the false negative predictions. The contour plots of $E(Q_c, T_c)$ are illustrated in panel D of Fig. 4 for one patient and in panel B, Fig. 5 for the collective data from 3 patients (total of 5 contacts). The error rate function is related to the accuracy function $A(Q_c, T_c) \equiv 1 - E(Q_c, T_c)$ that represents the relative number of correct predictions for a selected horizon and a given rPCI threshold.

3. Results

3.1. Interictal lateralization and localization

Inter-ictal localization and lateralization results are summarised in columns 1–5 of Table 1. The lateralization for all patients except patient 3 who was implanted only unilaterally, was done on the basis of the rPCI values collected interictally (>24 h before first seizure) from all left and right hippocampal contacts. The statistical test shows higher rPCI values measured from the SOS containing hemisphere in 4 out of 4 available cases (patients 1, 2, 4 and 5). In one case (patient 6) there was no early involvement of either hippocampi and the SOS was found outside the hippocampal areas. The median rPCI values from both hippocampi were relatively low in this case. For patients 1–5, a more detailed localization test was performed in order to select the precise contact, closest to the SOS. In all 5 cases the contact with highest rPCI was the same contact (patient 3) or one of the several contacts (patients 1, 2, 4, 5) where the SOS was identified by an ictal visual inspection. An optimal threshold value for the median interictal rPCI was selected so that the number of false positive and false negative SOS scores is minimal. The value was found to be close to 0.25 (see also Figs. 2 and 3) and it was used to separate the SOS from non-SOS and near-SOS sites in Table 1. Fig. 2 represents the interictal-rPCI statistics per trace in all patients separately. The overall classification power of the interictal rPCI is shown in Fig. 3 where the distributions of the median and mean rPCI values from all SOS, close to SOS and far from SOS traces (18 in total) are summarised.

3.2. Preictal anticipation

The seizure anticipation part of the study could be carried out only in 3 patients (patients 3, 4 and 5), since only in these cases we had sufficiently long periods of stimulations and analysis available. Patient 3 had 14 seizures within 52.4 h, the times of the follow-up seizures (presented as vertical red lines in Fig. 4A) were 4.0, 19.4, 20.6, 23.5, 24.4, 25.5, 28.5, 44.1, 44.9, 45.6, 46.6, 49.9 and 52.4 h after the pilot seizure. Patient 4 had 5 seizures within 23 h, with follow-up seizures at 10.3, 12.2, 19.1, 23.0 h after the leader seizure. From patient 5 only one seizure was recorded during our stimulation sessions. The associated statistical tests are illustrated in Fig. 4 (for patient 3, HCR 7 contact, 20 Hz stimulation). From panel D in this figure, one can use the error rate function (pseudo-colour coded) to chose for both a prediction horizon (vertical axis) and an optimal rPCI threshold (horizontal axis) that result in a minimal error rate. In this sense we do not prescribe in this work an absolute seizure-prediction horizon but rather define a procedure of selecting one with an optimal predictive power. Fig. 5 gives the statistics of times to the next seizure for all contacts that were found to produce rPCI with 'predictive power'. The non-linear association quantifiers measuring the 'predict-predictability' of seizures on basis of rPCI measurements are summarised in the last column of Table 1. For each patient the contact with the best score was selected. For patients 4 and 5 the contacts with highest predictive value were found to be in the contralateral side to the SOS. For patient 3 where no contralateral contacts were available, both SOS-hemisphere contacts gave good seizure predictability (0.713 at the SOS and 0.707 at the adjacent site). Finally Fig. 6 combines data from all contacts with statistically significant association between rPCI and time to seizure (marked with * in the last column of Table 1). From panel B, where the error rate of the total data set is plotted as function of an rPCI threshold and a selected prediction horizon, we see that 3 regions can be extracted. Values of rPCI>0.6 indicate in general immediate seizure (<2 h, more than 80% accuracy) while values between 0.1 and 0.3 indicate probable seizure expectancy within 10–30 h (>80% accuracy). Measured values of rPCI<0.1 statistically correlate with times to next seizure longer than 45 h (>80% accuracy).

4. Discussion

Theoretically, there is no principal argument imposing a deterministic relation between the brain's dynamics in its 'normal' state and the possibilities and features of an 'epileptic' state. Our previous studies (Lopes da Silva et al., 2003) have shown that bistable systems can exhibit both types of behaviour and switches between them can be due to noisy fluctuations. Such analysis, however, does not exclude indirect, possibly non-causal relations between interictal observable features and potential hazard of an ictal transition or seizure. We argue that such relation can be of a stochastic nature and it can provide statistical information on the most probable SOS in cases of early hippocampal involvement. In some cases the lack of large, asymmetric values of the rPCI can indicate extra-hippocampal SOS as demonstrated by the results from patient 6 (see Table 1, column 4). Time traces of rPCI can even give a probabilistic prognosis on the expected time to the next epileptic seizure. It is difficult, however, to draw general

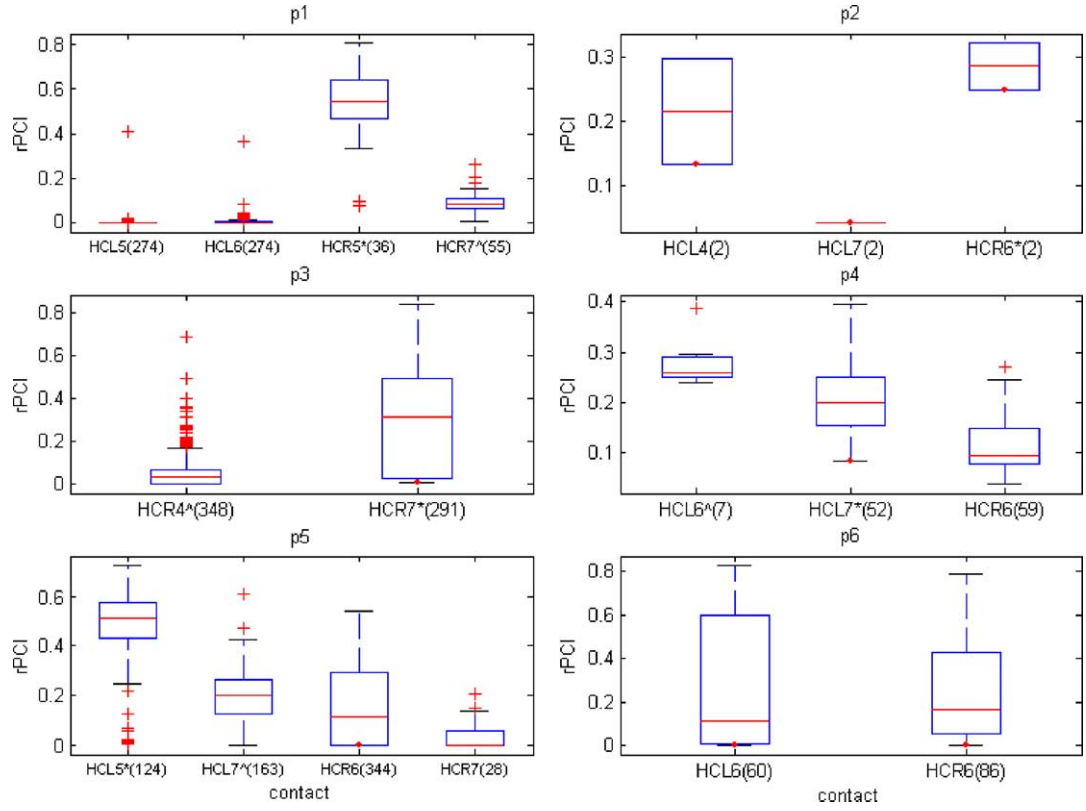

Fig. 2. Statistics of the lateralization and localization interictal rPCI measurements for all 6 patients. The box-plots give features of the rPCI distributions, the boxes extend from the 25 to the 75 percentiles and the whiskers extend to the rest the rPCI values. The horizontal lines represent the medial value and the outliers are marked with '+'. The horizontal axis indicates the electrode contact names and can be followed by * if the contact has been identified as unequivocal SOS from ictal EEG, or can be followed by ^ if the electrode contact has been found ipsilateraly near (but not at) the SOS. In brackets are indicated the number of measurement points that were available (>24 h before the first seizure) for this analysis.

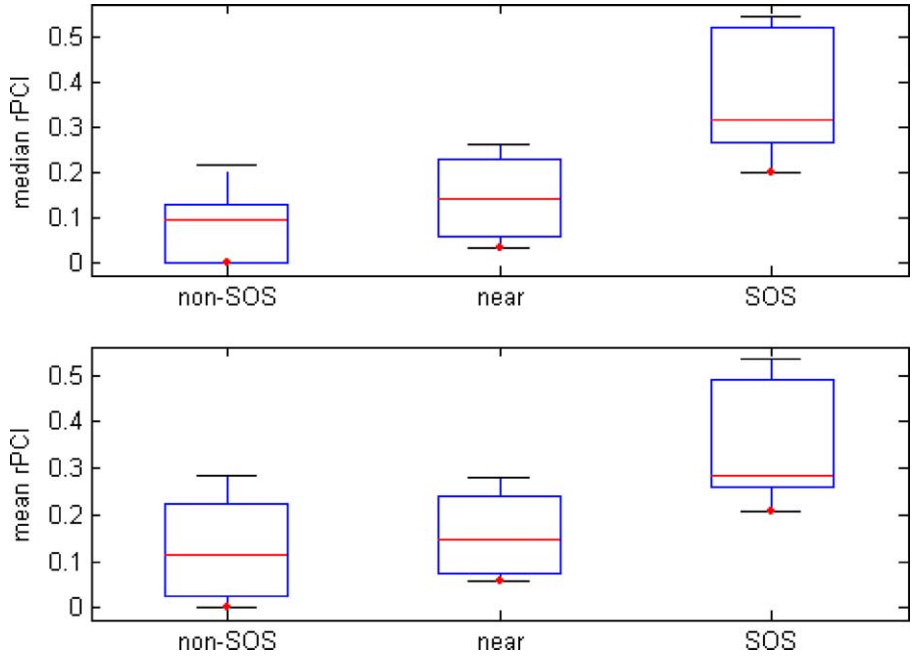

Fig. 3. Combined statistics (same notations as in Fig. 1) of the interictal rPCI values for all 18 traces of the 6 patients presented in this study. Median (upper plot) and mean (lower plot) interictal rPCI for each trace are computed and grouped according to SOS contacts, near contacts in the SOS-ipsilateral hemisphere and SOS-contralateral contacts (denoted as non-SOS), as found from ictal EEG. Threshold of median rPCI of 0.25 gives the optimal discrimination between SOS and non-SOS.

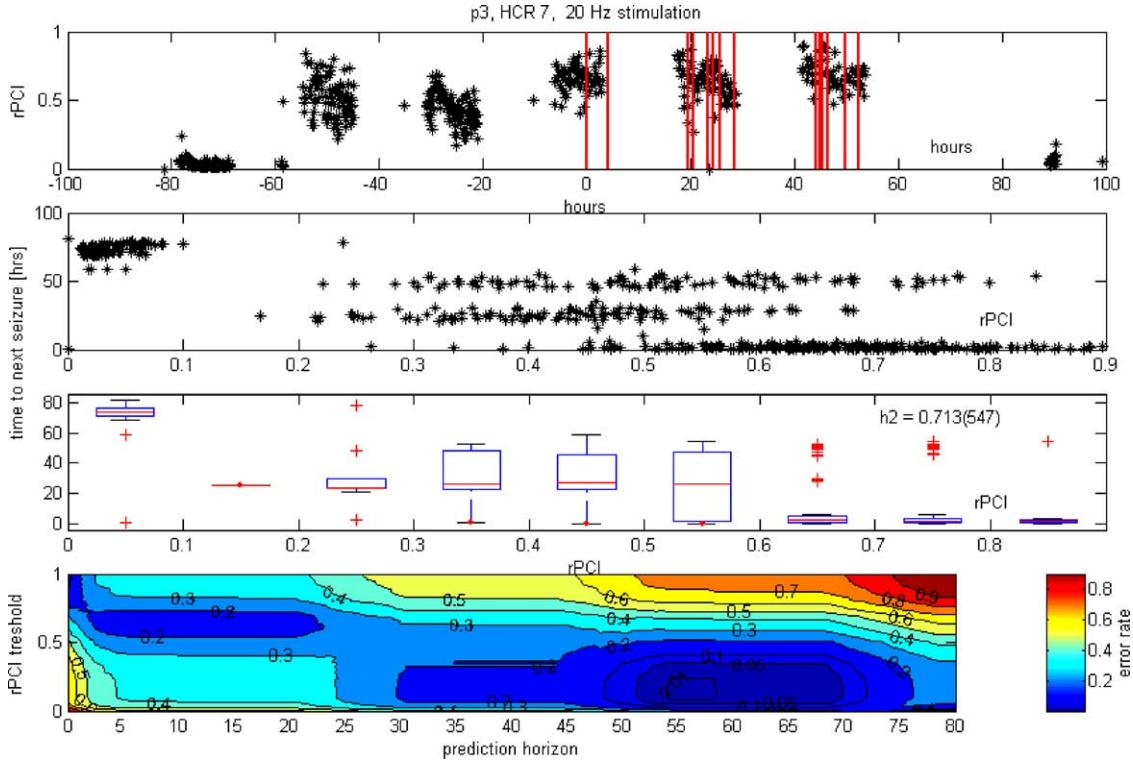

Fig. 4. rPCI 'en route' to a seizure (patient 3). Illustration of the 'seizure anticipation' features of the rPCI measurements. Panel A represents the time-course of the rPCI measured from a single hippocampal trace. Vertical lines indicate seizure-onsets, time (horizontal axis) is given in hours. The origin (time 0) of the time axis is conventionally set to the time of the patient's first EMU-recorded seizure (the so-called pilot seizure). Panel B represents a plot of rPCI values (horizontal axis) versus the time to the next following seizure (vertical axis, hours) for each measurement point. The patchy, inhomogenious structure of the plot is due to the fact that data were collected in this case mainly in the periods 08 pm–09 am (following day). On panel C the same information is represented in box-plots (same notations as in Fig. 1) where the rPCI values are divided in 10 bins of size 0.1. In the same panel the h^2 association value between the rPCI values and the times to next seizure is shown. The number in brackets following h^2 indicates the number of data points used. Panel D gives a pseudo-colour and contour plot of the prediction error rates defined in Section 2.4 as a function of the rPCI threshold (vertical axis) and the prediction horizon (in hours, horizontal axis).

conclusions from the above observations alone. Longer-term interictal measurements may change the statistical distributions of times to next seizure. The question of false positive statistics can only be fully addressed if longer periods of stimulation are available.

Another problem can be associated with possible non-stationarity of rPCI, although within the present statistical analysis we did not have to assume any stationary properties. Our patients were subjects, for example, to AED withdrawal so this inevitably leads to non-stationary EEG features, including the measured rPCI. The question then arises of whether the high rPCI values are not simply related to the medication withdrawal and therefore only indirectly related to the proximity in time to a seizure. The current study does not have enough power to answer this question with certainty. On the other hand, our patients were stimulated both during sleep and during wakefulness. We could identify no apparent correlation between the rPCI values and these two conditions. Therefore we may speculate that rPCI induced by intermittent electrical stimulation reflects local spatio-temporal tissue properties relevant for the ignition of epileptic activity much more than diurnal fluctuations can account for. At the same time our parallel measurements of the signal's power and mean frequency (not presented in this paper) showed clear cyclic behaviour correlated to the sleep pattern of the patient. The properties of rPCI may indicate the SOS and eventually, when spreading ipsi- or contralateraly, the probable timing of an ictal transition. The last observation suggests a possible 'recruitment' scenario for the seizure onset where specific network assemblies reach critical mass and trigger an ictal transition (Fig. 7).

The fact that in at least some of our patients seizure occurrence could be anticipated on the basis of increased rPCI measurements in the contralateral hippocampal formation corroborates evidence from previous studies. Interictal studies (Wilson et al., 1998) using the so-called paired pulse paradigm suggest that the contralateral hippocampal formation exhibits significantly less paired pulse suppression of population postsynaptic potentials than the SOS does. These authors attributed their findings to possibly adaptive enhanced inhibition suppressing seizures during interictal periods. Sabesan et al. (2003) reported changes in certain non-linear signal features (Lyapunov

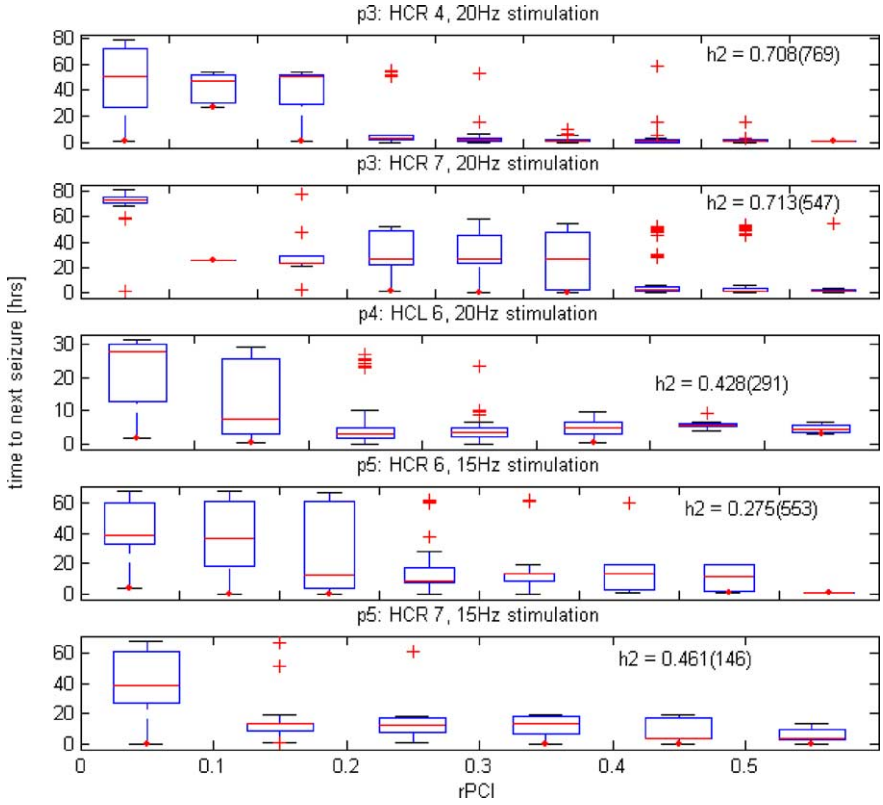

Fig. 5. rPCI 'en route' to a seizure, 3 patients. The same information as in panel C, Fig. 3 collected from all available sessions (marked with * in the last column of Table 1) that yielded statistically significant association between rPCI and the time to next seizure.

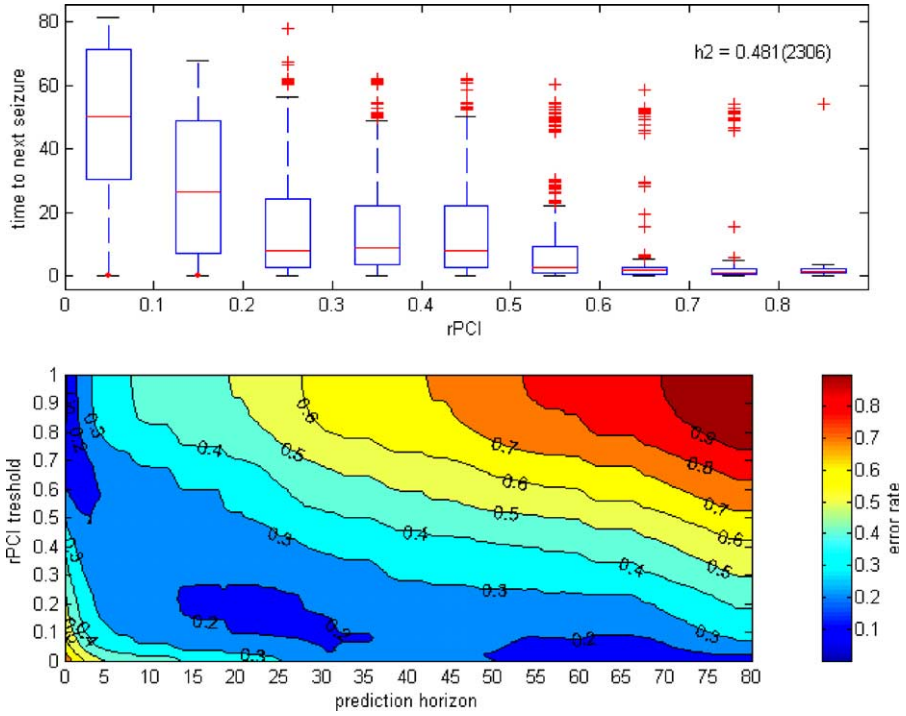

Fig. 6. rPCI 'en route' to a seizure combined for all sites. The two panels A and B show the same information as panels C and D correspondingly from Fig. 3 but for the combined rPCI and time-to-seizure statistics, collected from all contacts indicated with * in the last column of Table 1.

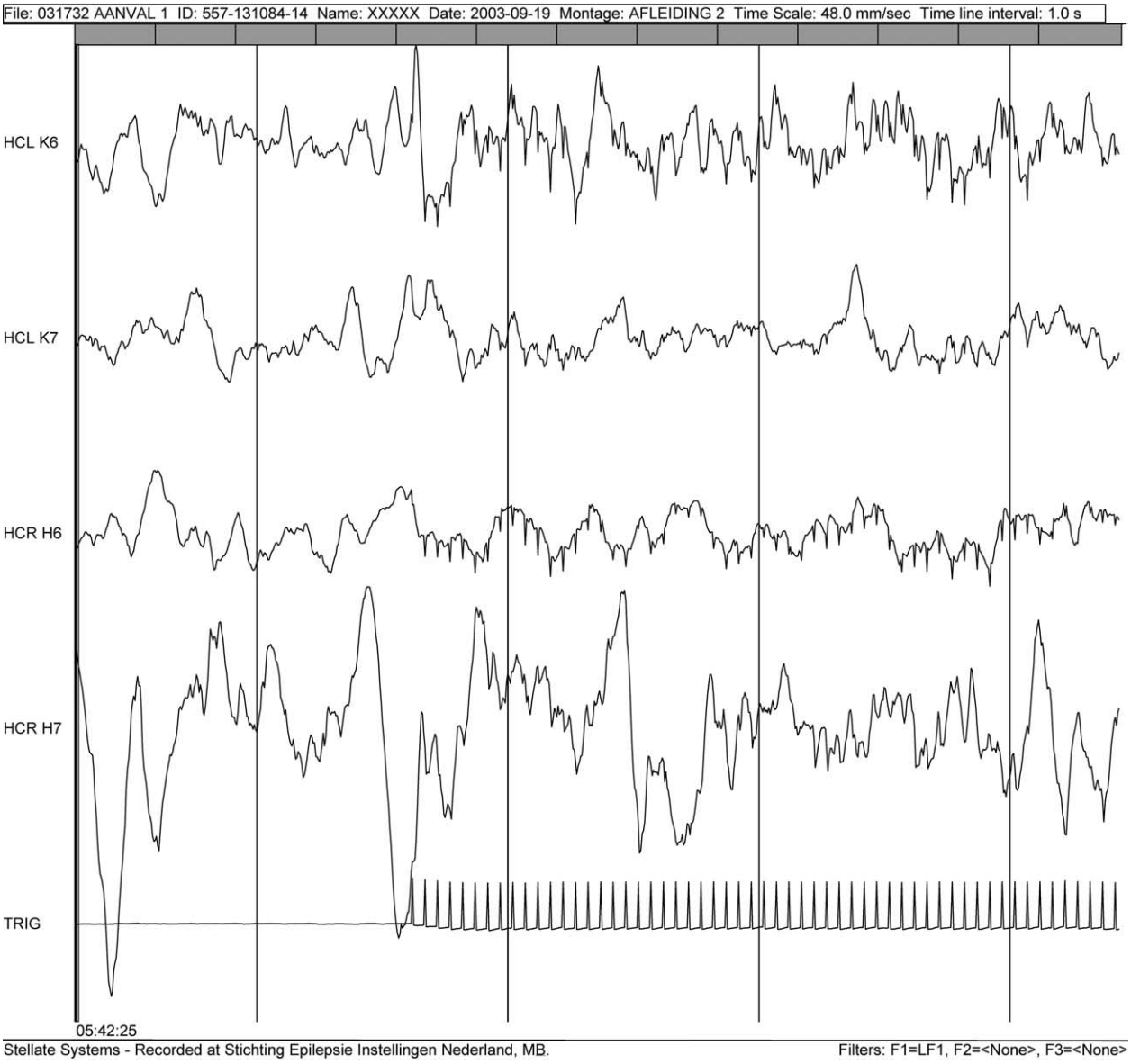

Fig. 7. Traces clipped from a of bilateral stimulation session. The stimulus was 20 Hz, 800 μA. Stimulated contacts are HCL K4, HCL K5, HCR H4 and HCR H5. All channels have the same sensitivity (15 μV/mm) and traces HCL K6 and HCR H6 that are closest to the stimulation contacts show stronger responses to the stimuli. The bottom trace represents the trigger signal.

exponents) measured from the contralateral site to the SOS. Similar findings based on a more general system-dynamics analysis can be found in Iasemidis et al. (2004). Changes in the cerebral blood flow in the contralateral hemisphere prior to seizures has been reported (Weinand et al., 2001). Viewed in this context early increased contralateral rPCI en route to a seizure might be an indication that an abnormal state of excitability leading to neuronal hypersynchronization might occur in the contralateral hippocampal formation as well.

The empirical data here presented constitute only a proof of principle for applying active stimulation paradigms in chronically implanted TLE cases. The fact that in our limited series seizure onset could be probabilistically anticipated gives an indication that rPCI measurements may be used to guide interventions with the aim of modifying local tissue excitability that ultimately might prevent the transition to a seizure. Further studies are warranted in establishing stimulation protocols 'on demand' for application in refractory (M)TLE cases.

Our protocol employs stimulation intensities that are below the threshold for evoking any visible after-discharges. Single-pulse stimulation of higher intensity and longer durations (4000 μA, 0.3–1 ms) can provoke early and delayed discharges (Valentin et al., 2002) the latter of which can be associated with the extend of neocortical excitability. Although in this work we have presented data from only hippocampal stimulation and recording, it may be

interesting to explore a connection between the subthreshold rPCI quantifier and the presence of afterdischarges in neocortical and/or hippocampal areas (Colder et al., 1996). Such a connection may yield more insights on the mechanisms responsible for high rPCI values in tissue close to the SOS.

We note that understanding the mechanisms relating interictally measured EEG features, such as rPCI, and the probability for an ictal transition can give important clues for possible dynamical scenarios that lead to epileptic seizure onsets. The very existence of a feature indicating 'closeness' to an ictal transition in a statistical context may indicate, for example, an essential 'random walk' component in the neuronal dynamics. In such a scenario, the system can drift closer to or further away from a transition threshold. Finally, one might speculate that a proper method for control of this state could be used to keep the system away from the ictal transition.

References

Aschenbrenner-Scheibe R, Maiwald T, Winterhalder M, Voss HU, Timmer J, Schulze-Bonhage A. How well can epileptic seizures be predicted? An evaluation of a nonlinear method Brain 2003;126:2616–26.

Colder BW, Wilson CL, Frysinger RC, Chao LC, Harper RM, Engel Jr J. Neuronal synchrony in relation to burst discharge in epileptic human temporal lobes. J Neurophysiol 1996;75:2496–508.

de Curtis M, Avanzini G. Interictal spikes in focal epileptogenesis. Prog Neurobiol 2001;63(5):541–67.

Dutch Collaborative Epilepsy Surgery Program. In: Engel Jr J, editor. Surgical treatment of the epilepsies. 2nd ed. New York: Raven Press; 1993. p. 711–2.

Gordon B, Lesser RP, Rance NE, Hart J, Webber Jr R, Uematsu S, Fisher RS. Parameters for direct cortical electrical stimulation in the human: histopathologic conformation. Electroencephalogr Clin Neurophysiol 1990;75:371–7.

Iasemidis LD. Epileptic seizure prediction and control. IEEE Trans Biomed Eng 2003;50(5):549–58.

Iasemidis LD, Shiau DS, Sackellares JC, Pardalos PM, Prasad A. Dynamical resetting of the human brain at epileptic seizures: application of nonlinear dynamics and global optimization techniques. IEEE Trans Biomed Eng 2004;51:493–506.

Kalitzin S, Parra J, Velis D, Lopes da Silva F. Enhancement of phase clustering in the EEG/MEG gamma frequency band anticipates transition to paroxysmal epileptiform activity in epileptic patients with known visual sensitivity. IEEE Trans Biomed Eng 2002;49(11):1279–86.

Lai YC, Harrison MA, Frei MG, Osorio I. Inability of Lyapunov exponents to predict epileptic seizures. Phys Rev Lett 2003;8:91–6.

Lehnertz K, Mormann F, Kreuz T, Andrzejak RG, Rieke C, David P, Elger CE. Seizure prediction by nonlinear EEG analysis. IEEE Eng Med Biol Mag 2003;22(1):57–63.

le Van Quyen M, Adam C, Martinerie J, Baulac M, Clemenceau S, Varela F. Spatio-temporal characterisation of non-linear changes in intracranial activities prior to human temporal lobe seizures. Eur J Neurosci 2000;12:21–4.

Lopes da Silva F, Pijn JP, Boeijinga P. Interdependence of EEG signals: linear vs. nonlinear associations and the significance of time delays and phase shifts. Brain Topogr 1989;2(1–2):9–18.

Lopes da Silva F, Blanes W, Kalitzin S, Parra J, Suffczynski P, Velis D. Dynamical diseases of brain systems: different routes to epilepsy. IEEE Trans Biomed Eng 2003;50(5):540–9.

Mormann F, Kreuz T, Andrzejak RG, David P, Lehnertz K, Elger CE. Epileptic seizures are preceded by a decrease in synchronization. Epilepsy Res 2003;53(3):173–285.

Parra J, Kalitzin S, Iriarte J, Blanes W, Velis D, Lopes da Silva F. Gamma band phase clustering and photosensitivity. Is there an underlying mechanism common to photosensitive epilepsy and visual perception? Brain 2003;126:1164–72.

Pijn JP, Vijn PC, Lopes da Silva FH, Van Ende Boas W, Blanes W. Localization of epileptogenic foci using a new signal analytical approach. Neurophysiol Clin 1990;20(1):1–11.

Sabesan S, Narayanan K, Prasad A, Spanias A, Sackellares JC, Iasemidis LD. Predictability of epileptic seizures: a comparative study using Lyapunov exponent and entropy based measures. Biomed Sci Instrum 2003;39:129–35.

Valentin A, Anderson M, Alarcon G, Seoane G, Selway R, Binnie CD, Polkey CE. Responses to single pulse electrical stimulation identify epileptogenesis in the human brain in vivo. Brain 2002;125:1709–18.

Van Emde Boas W, Velis DN, Brekelmans GJF, Van Veelen CWM. Temporal mesiolimbic versus temporal neocortical complex partial seizures; electroclinical correlates recorded by combined depth and subdural electrodes. Acta Neurol Scand 1990;82(suppl 133):22–3.

Van Veelen CWM, Debets RMC, Van Huffelen AC, Van Emde Boas W, Binnie CD, Storm Van Leeuwen W, Velis DN, Dieren A. Combined use of subdural and intracerebral electrodes in preoperative evaluation of epilepsy. Neurosurgery 1990;26:93–101.

Weinand ME, Labiner DM, Ahern GL. Temporal lobe seizure interhemispheric propagation time depends on nonepileptic cortical cerebral blood flow. Epilepsy Res 2001;44(1):33–9.

Wilson CL, Khan SU, Engel Jr J, Isokawa M, Babb TL, Behnke EJ. Paired pulse suppression and facilitation in human epileptogenic hippocampal formation. Epilepsy Res 1998;31:211–30.

Worrell GA, Parish L, Cranstoun SD, Jonas R, Baltuch G, Litt B. High-frequency oscillations and seizure generation in neocortical epilepsy. Brain 2004;127:1496–506.